Received: 7 March 2018 | Revised: 2 May 2018 | Accepted: 6 May 2018

DOI: 10.1002/aoc.4445

FULL PAPER

WILEY Applied Organometallic Chemistry

Anchoring Ni (II) on Fe_3O_4@tryptophan: A recyclable, green and extremely efficient magnetic nanocatalyst for one-pot synthesis of 5-substituted 1*H*-tetrazoles and chemoselective oxidation of sulfides and thiols

Nazanin Moeini[1] | Taiebeh Tamoradi[1] | Mohammad Ghadermazi[1] | Arash Ghorbani-Choghamarani[2]

[1]Department of Chemistry, Faculty of Science, University of Kurdistan, Sanandaj, Iran

[2]Department of Chemistry, Faculty of Science, Ilam University, PO Box 69315516, Ilam, Iran

Correspondence
Mohammad Ghadermazi, Department of Chemistry, Faculty of Science, University of Kurdistan, Sanandaj, Iran.
Email: mghadermazi@yahoo.com

A green, novel and extremely efficient nanocatalyst was successfully synthesized by the immobilization of Ni as a transition metal on Fe_3O_4 nanoparticles coated with tryptophan. This nanostructured material was characterized using Fourier transform infrared spectroscopy, transmission electron microscopy, scanning electron microscopy, energy-dispersive X-ray spectroscopy, thermogravimetric analysis, inductively coupled plasma optical emission spectroscopy, vibrating sample magnetometry and X-ray diffraction. The prepared nanocatalyst was applied for the oxidation of sulfides, oxidative coupling of thiols and synthesis of 5-substituted 1*H*-tetrazoles. The use of non-toxic, green and inexpensive materials, easy separation of magnetic nanoparticles from a reaction mixture using a magnetic field, efficient and one-pot synthesis, and high yields of products are the most important advantages of this nanocatalyst.

KEYWORDS
5-substituted 1*H*-tetrazoles, Fe_3O_4 nanoparticles, nickel, sulfides, thiols

1 | INTRODUCTION

Catalysis plays a crucial role in chemical processes, academic and industrial laboratories and various organic transformations. Recently, the applications of homogeneous catalysts in organic transformations have been limited because of difficulties in their recovery and reusability. For this reason, heterogeneous versions of catalysts can be used.[1] However, the activity of heterogeneous catalysts is less than that of their homogeneous counterparts. The solution to this problem is the use of the nanomaterials. Nowadays, nanoscale materials are used widely in sciences like chemistry, biology and physics.[2] Magnetic nanoparticles (MNPs) have attractive physical and chemical properties. Superparamagnetism, high magnetic susceptibility and low Curie temperature are some unique properties of MNPs.[3] Fe_3O_4 nanoparticles are a good candidate as a support material for heterogeneous catalysts because of their great properties such as the abundance of unique activities, low toxicity and price, simple synthesis and functionalization, large surface area and easy separation with magnetic field.[4–6] Fe_3O_4 has a cubic inverse spinel structure.[3] Magnetic nanocatalysts are used to accelerate various organic reactions.[7] Examples are the syntheses of compounds such as sulfoxides and disulfides, which are obtained from the oxidation of sulfides and oxidative coupling of thiols, respectively. Sulfoxides play a major role in the synthesis

of intermediates in drug metabolism, the production of biological compounds, industrial processes, C— C bond formation, etc.[8–10] The products of oxidative coupling of thiols are disulfides, having many valuable applications in organic synthetic chemistry as synthetic intermediates and are essential moieties in peptides and proteins.[11] Also, they are widely used in industry as vulcanizing agents and oils for rubber and elastomers.[12,13]

Tetrazoles are types of polyazaheterocyclic compounds.[14] They have widespread applications in medicine, materials science and coordination chemistry.[15] The [2 + 3] cycloaddition of azides to the corresponding nitriles in the presence of an appropriate catalyst is the best method for the synthesis of 5-substituted 1*H*-tetrazoles.[16] Transition metals play an important role as catalysts in synthesis of organic molecules. For instance, copper catalysts have been applied in the synthesis sulfoxides, disulfides and 5-substituted tetrazoles.[17–19] Corma and co-workers catalysed the oxidation of thiols to disulfides using gold nanoparticles.[20] Other reagents and catalysts are available for the oxidation of sulfides, such as PhIO/Mn (III) complexes,[21] vanadium (IV) complexes of dibromo- and diiodo-functionalized chiral Schiff bases[22] and magnesium monoperoxyphthalate.[23] But low selectivity which produces side products (sulfones), low yields, long reaction times and high cost of the reagents and catalysts are major disadvantages of these methods.[24] Fe $(OAc)_2$,[25] BF_3–OEt_2,[26] $FeCl_3$,[27] β-cyclodextrin[28] and ZnS nanospheres are several new catalysts that have been investigated for the synthesis of 5-substituted 1*H*-tetrazoles.[29]

Nickel is considered as one of the most effective transition metals for catalytic purposes in many synthetic transformations. Nickel is in group 10 of the periodic table, above palladium. It has chemical properties similar to those of palladium and platinum metals, with the advantages that it is cheaper, highly available, shows facile oxidative addition and is environmentally friendly.[30] Nickel-based catalysts are used in a large number of reactions: reductive coupling, cross-coupling, etc. The chemoselective oxidative coupling reaction of aliphatic thiols was reported as being catalysed by Ni nanoparticles.[31–33] In this regard, a magnetically recoverable nanohybrid catalyst containing nickel metal was synthesized. We report a facile method to synthesize Fe_3O_4@tryptophan@Ni as a heterogeneous and novel nanocatalyst for the synthesis of 5-substituted 1*H*-tetrazoles, the oxidative coupling of thiols and the oxidation of sulfides under mild conditions. The magnetic nanocatalyst was separated from reaction media using magnetic decantation. Also, the efficiency and reusability of the catalyst were evaluated.

2 | EXPERIMENTAL

2.1 | Materials and Instrumentation

Chemicals and solvents used in this work were obtained from Sigma-Aldrich and Merck. They were used without further purification. The particle size and morphology were examined using scanning electron microscopy (SEM) with a FESEM-TESCAN MIRA3. Fourier transform infrared (FT-IR) spectra of samples were recorded as KBr pellets with a Bruker Vertex 70 FT-IR spectrophotometer. ^{1}H NMR spectra were recorded with a Bruker 400 MHz NMR spectrometer. Transmission electron microscopy (TEM) was carried out with a Zeiss EM10C instrument. Powder X-ray diffraction (XRD) measurements were performed using a Philips X'pert diffractometer (Cu K αradiation, λ= 1.54060 Å). The content of Ni was measured using inductively coupled plasma optical emission spectrometry (ICP-OES). Thermogravimetric analysis (TGA) curves were obtained with a Shimadzu DTG-60 instrument. The supermagnetic properties of the catalyst were measured with vibrating sample magnetometry (VSM; MDKFD). Melting points were obtained usingan Electrothermal 9100 apparatus.

2.2 | Preparation of Fe_3O_4 MNPs

For preparation of Fe_3O_4 MNPs, 5.838 g of $FeCl_3 \cdot 6H_2O$ (0.022 mol) and 2.147 g of $FeCl_2 \cdot 4H_2O$ (0.011 mol) were dissolved in 100 ml of deionized water under a nitrogen atmosphere. Then, 10 ml of NH_3 was added to the reaction mixture and was stirred for 30 min at 80 °C. Finally, the black precipitate was isolated using an external magnet, washed several times with water and ethanol and dried at 50 °C.[34]

2.3 | Preparation of Fe_3O_4@tryptophan

An amount of 1 g of obtained Fe_3O_4 MNPs was dispersed in 250 ml of distilled water for 25 min. Then 2 mmol of tryptophan was added to the mixture and was refluxed for 24 h at 90 °C. The nanoparticle product (Fe_3O_4@tryptophan) was isolated by magnetic decantation, washed twice with deionized water and dried at room temperature.[35]

2.4 | Preparation of Fe_3O_4@tryptophan@Ni

An amount of 1 g of Fe_3O_4@tryptophan was dispersed in 25 ml of ethanol for 20 min. Subsequently, Ni $(NO_3)_2 \cdot 6H_2O$ (2 mmol) was added to the suspension. The resultant mixture was refluxed for 15 h. The

synthesized Fe_3O_4@tryptophan@Ni was decanted from the reaction mixture using a magnetic field, washed with ethanol and dried at room temperature.

2.5 | Procedure for Oxidation of Sulfides to Sulfoxides

To a mixture of 1 mmol of sulfide and 0.4 ml of H_2O_2 (33%), 0.004 g of nanocatalyst was added (amount of anchored Ni in 4 mg of catalyst: 0.0006 mmol g^{-1}) and stirred at room temperature for a specified time. TLC was used to evaluate the reaction progress. Fe_3O_4@tryptophan@Ni nanocatalyst was isolated using an external magnet when reaction had completed and the resulting mixture was washed with ethyl acetate. Finally, pure sulfoxides were obtained in high yields (80–99%) after solvent evaporation.[36]

2.6 | Procedure for Oxidative Coupling of Thiol to Disulfide

A mixture containing 1 mmol of thiol, 0.4 ml of H_2O_2 (33%), 0.004 g of Fe_3O_4@tryptophan@Ni catalyst (amount of anchored Ni in 4 mg of catalyst: 0.0006 mmol g^{-1}) and 2 ml of ethanol as a solvent was stirred at room temperature. The reaction process was monitored by TLC. After the reaction was complete, the magnetic nanocatalyst was removed by magnetic separation and the product was washed with ethyl acetate. After evaporation of ethyl acetate, the corresponding pure disulfides were obtained in high yields (85–99%).[37]

2.7 | Procedure for Synthesis of 5-Substituted 1*H*-Tetrazole Derivatives

A mixture of 1 mmol of nitrile, 1 mmol of sodium azide and 0.08 g of the nanocatalyst (amount of anchored Ni in 0.08 g of catalyst: 0.0122 mmol g^{-1}) in 1 ml of poly (ethylene glycol) (as green solvent) was stirred at 120 °C. TLC was used for indicating completion of the reaction. After the reaction was cooled, the nanocatalyst was separated from the resultant material using a magnetic field. Then, 10 ml of hydrochloric acid (4 N) was added and ethyl acetate was used for extracting the tetrazole. The organic part was separated from the water part and concentrated to form crude crystalline solid.[38]

2.8 | Selected Spectral Data

Methylphenylsulfoxide. ^{1}H NMR (400 MHz, $CDCl_3$, δ_H, ppm): 2.74 (s, 3H), 7.00–7.99 (m, 5H). FT-IR (KBr, cm^{-1}): ν (S═ O): 1026–1089.

2,2′-Disulfanediyldisuccinic acid. ^{1}H NMR (400 MHz, DMSO, δ_H, ppm): 2.59 (s, 4H), 6.89 (br, 4H). FT-IR (KBr, cm^{-1}): ν (S— S): 1043.

1,2-Di-*p*-tolyldisulfane. ^{1}H NMR (400 MHz, DMSO, δ_H, ppm): 2.30 (s, 6H), 6.74–6.81 (m, 4H), 7.74–7.98 (m, 4H). FT-IR (KBr, cm^{-1}): ν (S— S): 1034.

2-(1*H*-Tetrazol-5-yl)phenol. ^{1}H NMR (400 MHz, DMSO, δ_H, ppm): 6.99–7.03 (t, J = 7.4, 1H), 7.09 (d, J = 8, 1H), 7.39–7.43 (t, J = 7.6, 1H), 8.01 (d, J = 8, 1H), 13.05 (br, 1H). FT-IR (KBr, ν_{max}, cm^{-1}): 3233, 3029, 2923, 2710, 2520, 2400, 1600, 1555, 1465, 1392, 1355, 1275, 1250, 1110, 1056, 899, 810, 732, 685, 550.

4-(1*H*-Tetrazol-5-yl)benzonitrile. ^{1}H NMR (400 MHz, DMSO, δ_H, ppm): 8.09–8.21 (m, 2H), 8.21–8.23 (m, 2H). FT.IR (KBr, ν_{max}, cm^{-1}): 3394, 3095, 3050, 2877, 2859, 2737, 2624, 2565, 2480, 2230, 1618, 1566, 1494, 1457, 1353, 1227, 1115, 1071, 997, 886, 757, 698, 559.

3 | RESULTS AND DISCUSSION

The synthesis of the new MNPs was realized by attaching tryptophan to the Fe_3O_4 nanomagnetic substrate. Ultimately, the Fe_3O_4@tryptophan@Ni nanocatalyst was prepared using a stable interaction between the N atom (primary amine) of tryptophan and Ni^{2+} (Scheme 1).

3.1 | Catalyst Characterization

The FT-IR spectra confirm the successful functionalization of the MNPs. Figure 1 shows the FT-IR spectra for Fe_3O_4 MNPs, Fe_3O_4@tryptophan and Fe_3O_4@tryptophan@Ni. A strong peak near 578 cm^{-1} is seen in Figure 1(a), which verifies the existence of the Fe— O bond and is evidence for the synthesis of Fe_3O_4 MNPs.[39] The FT-IR spectra of Fe_3O_4@tryptophan (Figure 1b) and Fe_3O_4@tryptophan@Ni (Figure 1c) show the band of the bending vibration of NH_2 near 1400 cm^{-1} this band is shifted to lower wavenumber in the spectrum of Fe_3O_4@tryptophan@Ni because of coordination of nitrogen atom of the amino group to nickel.[40] The FT-IR spectrum of Fe_3O_4@tryptophan shows an NH_2 stretching band near 3250 cm^{-1} while in the Fe_3O_4@tryptophan@Ni spectrum this is shifted to 3236 cm^{-1}.[41] All of these bands indicate that the surface of Fe_3O_4 MNPs is successfully modified with tryptophan and Ni (II) immobilized on Fe_3O_4@tryptophan.

The thermal stability of Fe_3O_4@tryptophan@Ni nanoparticles was investigated using TGA from 35 to 635 °C. The overlaid TGA curves of Fe_3O_4 nanoparticles, Fe_3O_4@tryptophan and Fe_3O_4@tryptophan@Ni are shown in Figure 2. The removal of solvent, physically adsorbed water and surface hydroxyl groups was detected

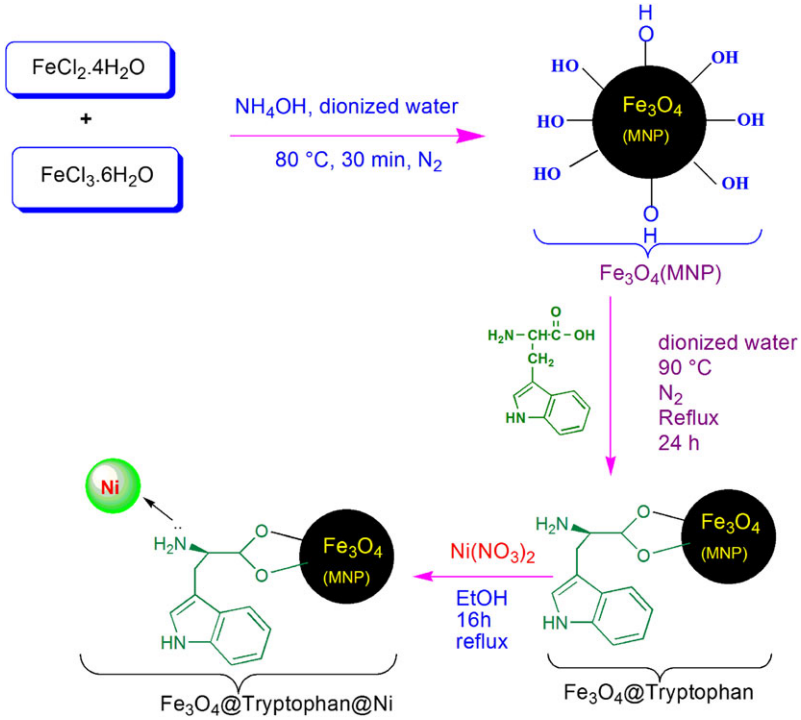

SCHEME 1 Synthesis of Fe_3O_4@tryptophan@Ni

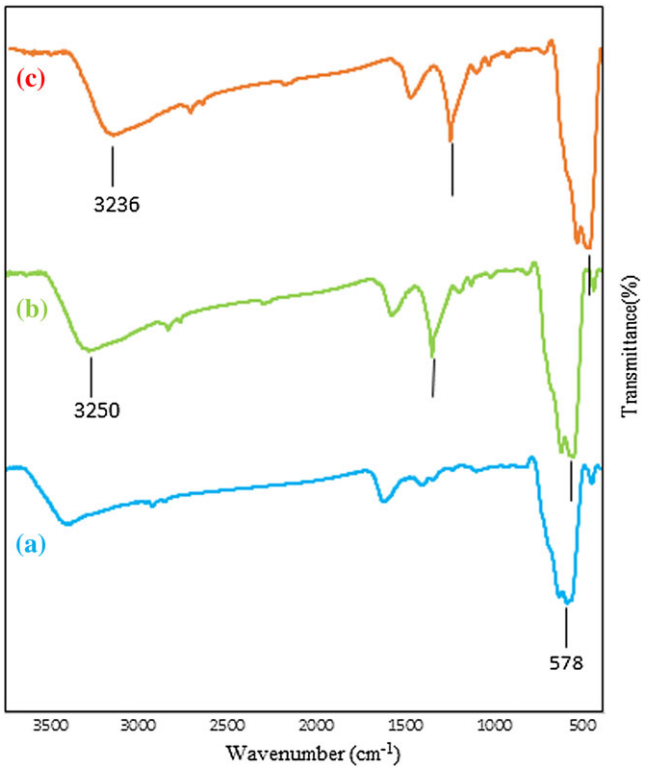

FIGURE 1 FT-IR spectra of (a) Fe_3O_4 nanoparticles, (b) Fe_3O_4@tryptophan and (c) Fe_3O_4@tryptophan@Ni

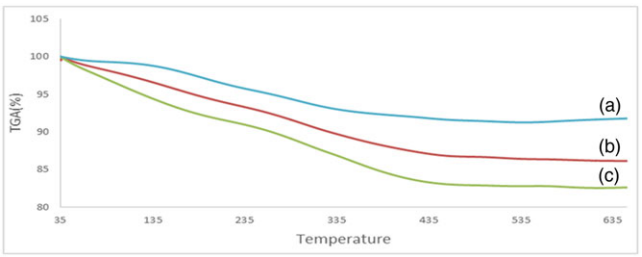

FIGURE 2 TGA curves of (a) Fe_3O_4 nanoparticles, (b) Fe_3O_4@tryptophan and (c) Fe_3O_4@tryptophan@Ni

by the decrease in the mass in the region below 200 °C.[42] A weight decrease at 250–635 °C corresponds to the decomposition of the organic substance on the substrate of MNPs.

The crystalline structures of synthesized Fe_3O_4 MNPs, Fe_3O_4@tryptophan and Fe_3O_4@tryptophan@Ni were analysed using XRD (Figure 3). The pattern of Fe_3O_4 MNPs indicates a crystallized structure with peaks at 2θ= 30.37°, 35.82°, 43.25°, 53.92°, 57.39° and 62.77°, assigned to the crystallographic faces (2 2 0), (3 1 1), (4 0 0), (4 2 2), (5 1 1) and (4 4 0), which is indicative of an inverse cubic spinel structure.[43] The Fe_3O_4@tryptophan@Ni phase was identified by the peak positions at 2θvalues of 29.99°, 35.76°, 43.25°, 53.89°, 57.15° and 62.61°. The XRD patterns of Fe_3O_4@tryptophan and Fe_3O_4@tryptophan@Ni clearly showed that these modifications did not cause a phase change during the synthesis of the nanocatalyst and the structure was retained.

As shown in Figure 4, the size and morphology of Fe_3O_4@tryptophan@Ni nanocatalyst were investigated using SEM. According to the SEM images, spherical morphology was observed for most particles. A TEM image of the Fe_3O_4@tryptophan@Ni catalyst is shown in Figure 5. The particle size was measured to be about 15 nm and

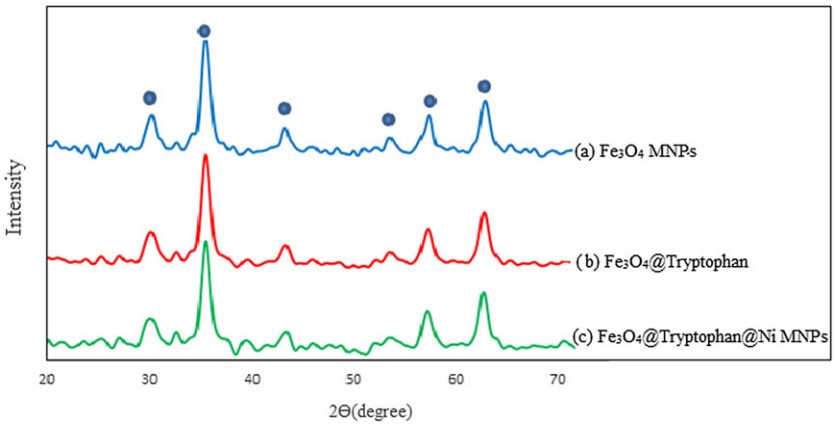

FIGURE 3 XRD patterns of (a) Fe_3O_4 MNPs, (b) Fe_3O_4@tryptophan and (c) Fe_3O_4@tryptophan@Ni MNPs

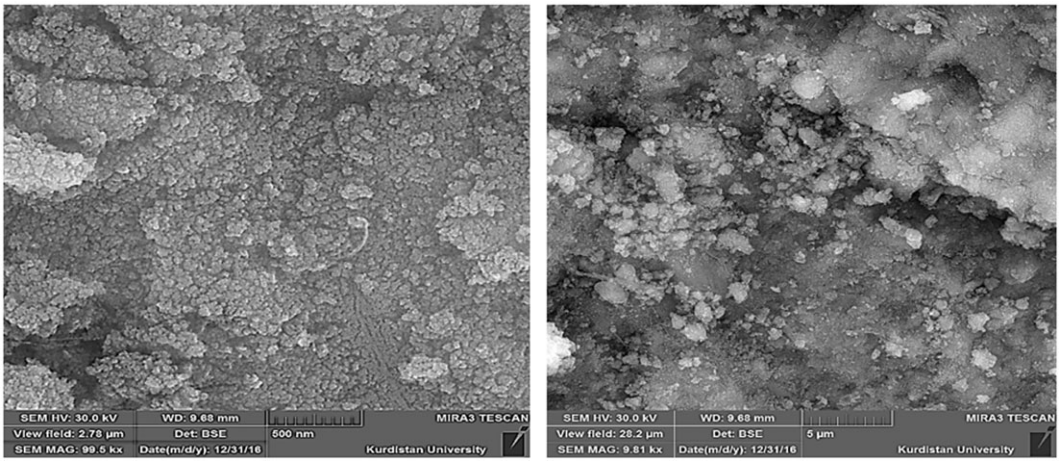

FIGURE 4 SEM images of Fe_3O_4@tryptophan@Ni at different magnifications

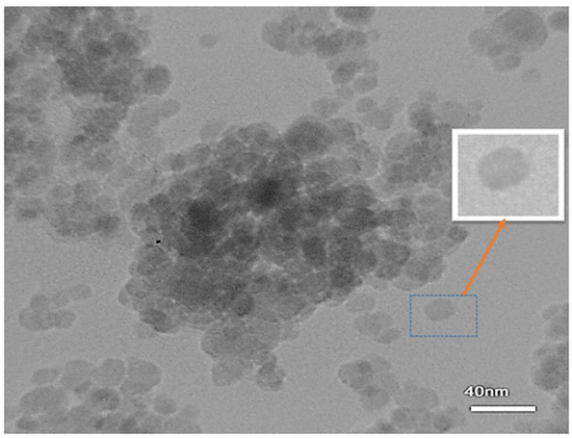

FIGURE 5 TEM image of Fe_3O_4@tryptophan@Ni catalyst

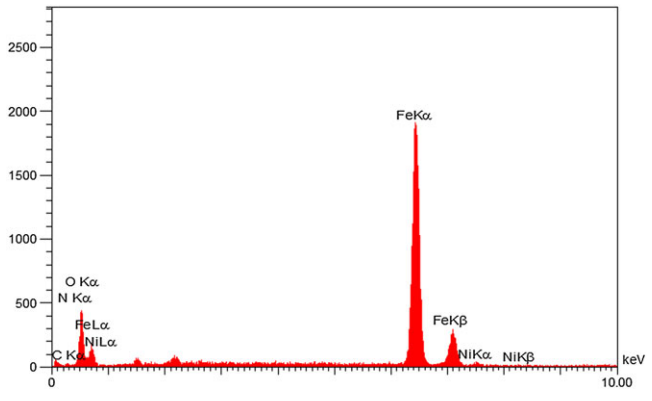

FIGURE 6 Energy-dispersive X-ray spectrum of Fe_3O_4@tryptophan@Ni

spherical morphology was confirmed. The results of TEM and SEM were in agreement.

The components of Fe_3O_4@tryptophan@Ni were investigated using energy-dispersive X-ray spectroscopy (Figure 6). The results showed that the main elements were C, N, O, Fe and Ni, which established that tryptophan was well attached to the Fe_3O_4 substrate.

The magnetic properties of Fe_3O_4, Fe_3O_4@tryptophan and Fe_3O_4@tryptophan@Ni were evaluated using VSM at room temperature (Figure 7). The saturation magnetization value (M_s) of the Fe_3O_4 MNPs was found to be 66.87 emu g^{-1} and those for Fe_3O_4@tryptophan and Fe_3O_4@tryptophan@Ni composite were 47.83 and 42.95 emu g^{-1}, respectively. As shown in Figure 7, the

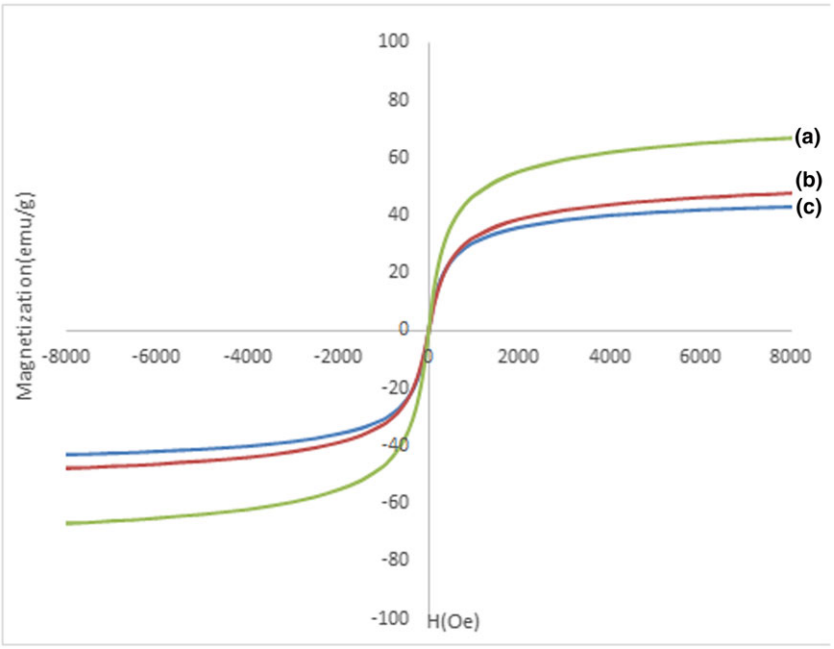

FIGURE 7 VSM curves of (a) Fe_3O_4, (b) Fe_3O_4@tryptophan and (c) Fe_3O_4@tryptophan@Ni MNPs

decline in the magnetization of the nanocatalyst relative to the Fe_3O_4 MNPs is related to the coating of the Fe_3O_4 MNPs with the organic layers (tryptophan) and coordination with nickel.[38] Nonetheless, this magnetic property is sufficient and the Fe_3O_4@tryptophan and Fe_3O_4@tryptophan@Ni nanoparticles could be completely, efficiently and rapidly separated using a magnet from reaction mixtures.

The amount of anchored Ni on the nanoparticles was determined using ICP-OES. The value was 0.152 mmol g^{-1}.

3.2 | Catalytic Studies

Application of Fe_3O_4@tryptophan@Ni nanocatalyst in the oxidation of sulfides to sulfoxides, in the oxidative coupling of thiols to disulfides and also in the synthesis of tetrazole derivatives was studied. Different amounts of the catalyst, H_2O_2 and various solvents were investigated using methylphenylsulfide (as a model compound) to obtain the optimized conditions for oxidation of sulfides (Scheme 2). The results are summarized in Table 1. In the absence of the catalyst, even after 120 min, the desired product was not obtained. Therefore, this showed evidence of the efficiency of the synthesized nanocatalyst in this reaction. The optimized conditions were found to be 0.4 ml of hydrogen peroxide, solvent-free condition, 4 mg

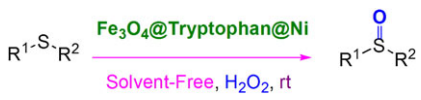

SCHEME 2 Oxidation of sulfides to sulfoxides

TABLE 1 Optimization of oxidation of sulfides catalysed by Fe_3O_4@tryptophan@Ni under various conditions

Entry	Solvent	H_2O_2 (ml)	Catalyst (mg)	Time (min)	Yield (%)
1	Solvent-free	0.4	0	120	10
2	Solvent-free	0.4	3	24	80
3	Solvent-free	0.4	4	20	98
4	Solvent-free	0.4	6	15	98
5	Solvent-free	0.2	4	40	90
6	Solvent-free	0.1	4	100	52
7	Solvent-free	0.6	4	20	95
8	EtOH	0.4	4	135	75
9	Ethyl acetate	0.4	4	960	45
10	Acetonitrile	0.4	4	1800	20

of Fe_3O_4@tryptophan@Ni at room temperature (Table 1, entry 3).

Therefore, after finding the optimal conditions, various derivatives of sulfides were evaluated. The results are presented in Table 2. The best yields were obtained in short times in the presence of the nanocatalyst for oxidation of various sulfides.

All corresponding sulfoxides were obtained in excellent yields within a relatively short period of time. Selectivity is one of the most important features in catalytic systems. The reaction of the oxidation of sulfides with the optimized conditions described previously is completely selective. Therefore in these reactions, sulfone was not seen as a by-product. A possible reaction mechanism for the oxidation of sulfides in the presence of the

TABLE 2 Oxidation of sulfides to sulfoxides in the presence of Fe_3O_4@tryptophan@Ni

Entry	Substrate	Time (min)	Yield (%)	M.p. (°C)
1	2-(Phenylthio)ethanol	5	99	Oil[27]
2	Dibenzylsulfide	6	92	140–143[34]
3	2-(Methylthio)ethanol	5	94	Oil[27]
4	Dodecylmethylsulfide	5	80	60–63[41]
5	Allyl sulfide	5	82	Oil[42]
6	3,3′-Thiodipropionic acid	5	94	205–210
7	Dipropylsulfide	5	85	Oil[42]
8	Methylphenylsulfide	20	98	Oil[27]
9	Thiodiglycolic acid	6	98	160–175
10	Ethylphenylsulfide	25	96	Oil[27]

catalyst is shown in Scheme 3. The reaction of hydrogen peroxide with the catalyst produces intermediate A, which converts to active oxidant B. Subsequently, sulfide with a nucleophilic attack on intermediate C leads to the production of sulfoxide.[44]

Also, we decided to examine the oxidative coupling of thiols to corresponding disulfides (Scheme 4). Mercaptosuccinic acid was selected as a model to optimize the reaction conditions. Oxidation reactions were performed in several solvents, various amounts of Fe_3O_4@tryptophan@Ni catalyst and H_2O_2. Amounts of 4 mg of the catalyst and 0.4 ml of H_2O_2 in 2 ml of ethanol were optimal conditions for the reaction (Table 3). The reaction was investigated in the absence of the catalyst. Low yield and a long reaction time in the absence of

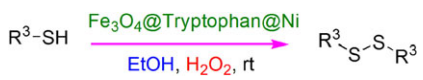

SCHEME 4 Oxidative coupling of thiols to disulfides

TABLE 3 Optimization of oxidation of thiols catalysed by Fe_3O_4@tryptophan@Ni under various conditions

Entry	Solvent	H_2O_2 (ml)	Catalyst (mg)	Time (min)	Yield (%)
1	EtOH	0.4	0	60	14
2	EtOH	0.4	3	5	92
3	EtOH	0.4	4	5	97
4	EtOH	0.4	6	4	99
5	EtOH	0.2	4	14	90
6	EtOH	0.6	4	5	98
7	EtOH	0.1	4	55	49
8	Solvent-free	0.4	4	20	88
9	Ethyl acetate	0.4	4	13	90
10	Acetonitrile	0.4	4	110	77

the catalyst show the positive effect of the catalyst on the reaction.

Then, ten substrate thiols were converted to the desired disulfides under the optimal conditions. As evident from Table 4, the oxidative coupling of thiols in the presence of the nanoparticles occurred in the desired times and with good yields. A plausible mechanism for this process is shown in Scheme 5.[48]

The chemoselectivity of substrates containing a hydroxyl group (2-(phenylthio) ethanol, 2-(methylthio)

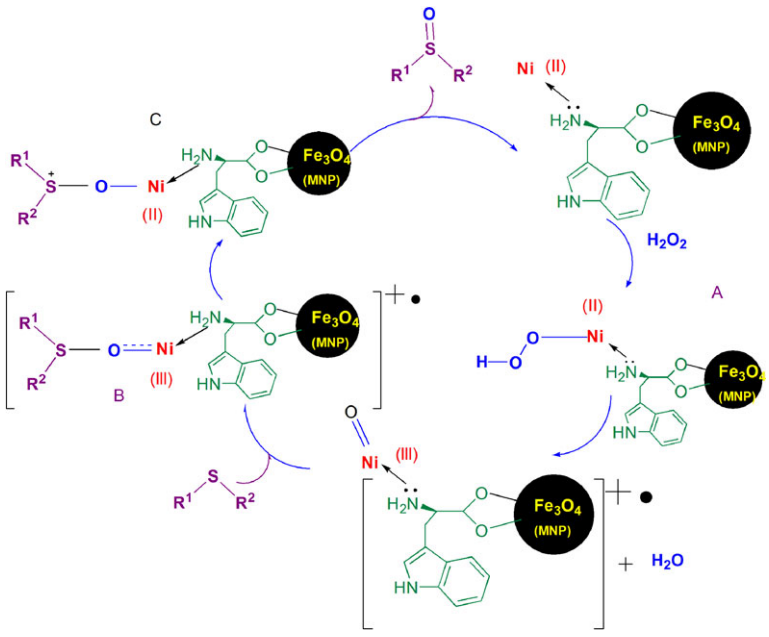

SCHEME 3 Possible reaction mechanism for oxidation of sulfides in the presence of the catalyst

TABLE 4 Oxidative coupling of thiols catalysed by Fe_3O_4@tryptophan@Ni under various conditions

Entry	Substrate	Time (min)	Yield (%)	M.p. (°C)
1	2-Mercaptoethanol	5	98	Oil[41]
2	Mercaptosuccinic acid	5	99	105–110[17]
3	2-Mercaptobenzoic acid	15	98	270–272[41]
4	2-Mercaptobenzimidazole	60	86	195–197[45]
5	Thiophenol	65	87	55–57[46]
6	Benzylmercaptan	55	96	7072[47]
7	Benzo [*d*]thiazole-2-thiol	50	88	169–170[34]
8	Benzo [*d*]oxazole-2-thiol	180	85	98–99[34]
9	4-Methylbenzenethiol	60	96	38–40[34]
10	2-Mercaptoacetic acid	10	85	Oil[41]

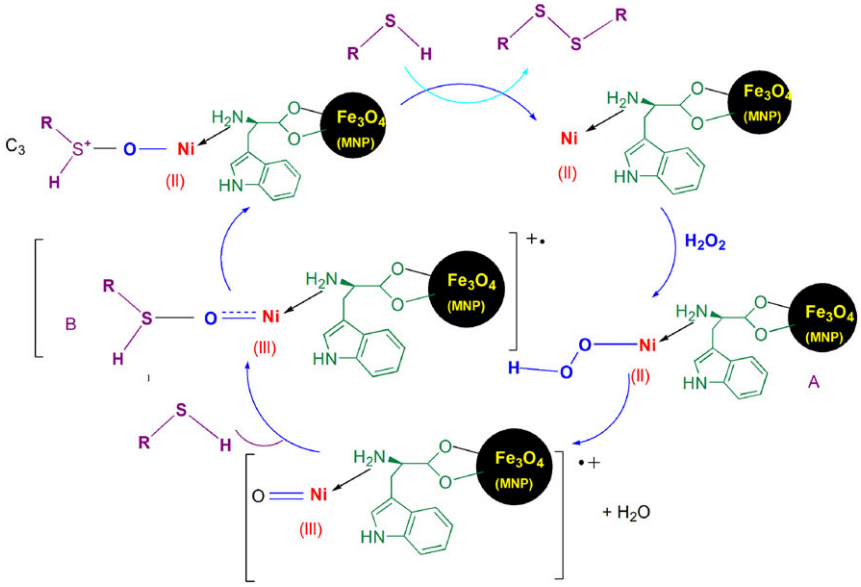

SCHEME 5 Plausible mechanism for oxidative coupling of thiols to corresponding disulfides

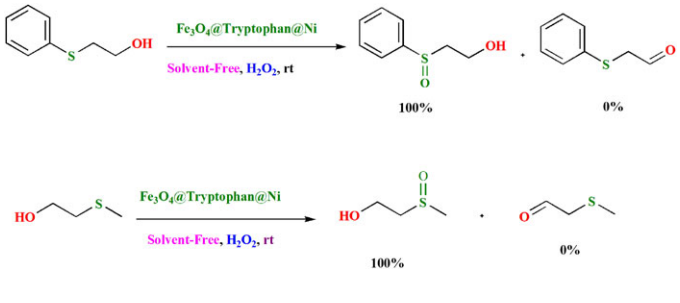

SCHEME 6 Chemoselective sulfoxidation of 2-(phenylthio) ethanol and 2-(methylthio)ethanol

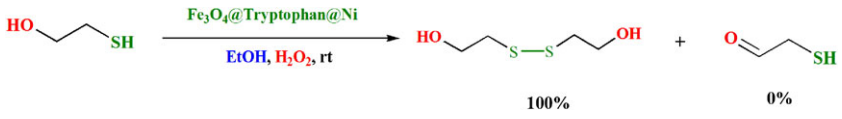

SCHEME 7 Chemoselective sulfoxidation of 2-mercaptoethanol

ethanol and 2-mercaptoethanol) in the oxidation of sulfide and thiol was investigated. In these oxidation reactions, as shown in Schemes 6 and 7, hydroxyl group remained intact and functional groups of sulfide and thiol were oxidized to sulfoxide and disulfide, respectively.

Finally, the catalytic effect of Fe_3O_4@tryptophan@Ni on the synthesis of tetrazoles was investigated (Scheme 8). Initially, to optimize the reaction conditions, malononitrile was selected and studied in the presence of various amounts of Fe_3O_4@tryptophan@Ni, several solvents and at different temperatures. As evident from Table 5, the appropriate outcomes) 0.08 g of Fe_3O_4@tryptophan@Ni and poly (ethylene glycol) (PEG) as a green solvent instead of dimethylformamide (DMF) at 120 °C (were obtained. Also, the reaction proceeds in the absence of the catalyst.

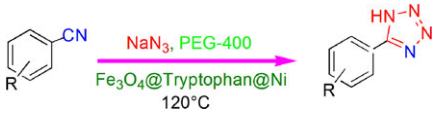

SCHEME 8 Synthesis of tetrazoles

Various derivatives of nitriles were evaluated under the optimized conditions. The results are presented in Table 6.

3.3 | Reusability and Leaching of Catalyst

Reusability is one of the most important advantages of catalysts that makes them economically efficient. The recyclability of Fe_3O_4@tryptophan@Ni was assessed. We used the separated nanocatalyst for nine, seven and five runs in the oxidative coupling of thiols, oxidation of sulfides and synthesis of 5-substituted 1*H*-tetrazoles, respectively, without a significant decrease in activity of subsequent runs, as shown in Figure 8.

In order to investigate the leaching of nickel from Fe_3O_4@tryptophan@Ni in the synthesis of methylphenylsulfoxide, the exact amount of Ni loaded on modified MNPs was analysed using the ICP-OES technique for recycled and fresh nanocatalyst. The amounts

TABLE 5 Optimization of formation of 5-(4-chlorophenyl)-1*H*-tetrazole catalysed by Fe_3O_4@tryptophan@Ni under various conditions

Entry	Solvent	Temperature (°C)	Catalyst (g)	Time (min)	Yield (%)
1	EtOH	80	0.08	1440	22
2	DMF	120	0.08	150	60
3	DMSO	120	0.08	180	55
4	PEG	120	0.08	20	97
5	PEG	100	0.08	150	85
6	PEG	80	0.08	195	70
7	PEG	120	0.06	30	85
8	PEG	120	0.05	90	72
9	PEG	120	0	300	16

TABLE 6 Synthesis of 5-substituted 1*H*-tetrazoles in the presence of Fe_3O_4@tryptophan@Ni in PEG

Entry	Substrate	Time (min)	Yield (%)	M.p. (°C)
1	Phthalonitrile	5	97	209–213[49]
2	3-Nitrobenzonitrile	480	89	141–145[49]
3	2-Chlorobenzonitrile	327	91	175–180[49]
4	Malononitrile	20	97	110–112[49]
5	4-Nitrobenzonitrile	25	97	215–218[49]
6	Benzonitrile	15	98	210–215[49]
7	Benzyl cyanide	20	88	122–125[49]
8	2-Hydroxybenzonitrile	10	97	220–223[50]
9	3-Chlorobenzonitrile	5	98	265–268[49]
10	Terephthalonitrile	30	91	195–200[51]

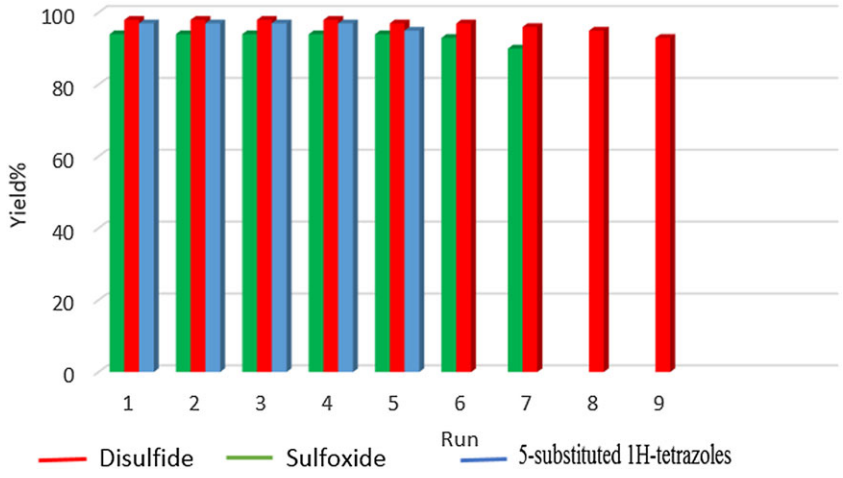

FIGURE 8 Reuse of the nanocatalyst in oxidative coupling of thiols, oxidation of sulfides and synthesis of 5-substituted 1*H*-tetrazoles

TABLE 7 Comparison of Fe_3O_4@tryptophan@Ni for oxidation of methylphenylsulfide with previously reported catalysts

Entry	Substrate	Catalyst	Time (min)	Yield (%)
1	Ph–SCH_3	Cu-SPATB/Fe_3O_4	95	98[29]
2	Ph–SCH_3	Ni–salen–MCM-41	156	95[43]
3	Ph–SCH_3	Fe_3O_4–adenine–Ni	55	98[41]
4	Ph–SCH_3	Polymer-anchored Cu (II)	180	90[44]
5	Ph–SCH_3	Cd–salen–MCM-41	150	98[47]
6	Ph–SCH_3	Fe_3O_4@tryptophan@Ni	20	98 (this work)
7	4-Methylbenzenthiol	Ni-SMTU@boehmite	93	94[52]
8	4-Methylbenzenthiol	Fe_3O_4-adenine-Zn	90	99[38]
9	4-Methylbenzenthiol	Fe_3O_4-adenine-Ni	70	97[41]
10	4-Methylbenzenthiol	Fe_3O_4@tryptophan@Ni	60	96 (this work)
11	Benzonitrile	Ni–SMTU@boehmite	93	94[49]
12	Benzonitrile	Fe_3O_4@SiO2@L-histidine	180	90[53]
13	Benzonitrile	Pd-2A3HP-MCM-41	180	94[54]
14	Benzonitrile	Cuttlebone	20	98[55]
15	Benzonitrile	Fe_3O_4@tryptophan@Ni	15	98 (this work)

of nickel in the recycled and fresh catalysts were 0.10 and 0.152 mmol g^{-1}, respectively.

3.4 | Comparison of Catalysts

The catalytic activity of Fe_3O_4@tryptophan@Ni was compared with that of other materials. The results summarized in Table 7 show that oxidations of methylphenylsulfide, 4-methylbenzenthiol and benzonitrile occur in the presence of Fe_3O_4@tryptophan@Ni in a shorter time period and with higher yields than in the presence of the other catalysts. Non-toxicity of ligand and metal in the catalyst, magnetic and easy separation of nanohybrid catalyst, commercially available materials, high yields and short reaction times are several advantages of this synthesized nanomagnetic catalyst.

4 | CONCLUSIONS

Ni (II) immobilized on Fe_3O_4 nanoparticles coated with tryptophan was prepared as a novel, green, inexpensive and efficient magnetic nanocatalyst. The nanostructure was characterized using TGA, ICP-OES, FT-IR, energy-dispersive X-ray spectroscopy, XRD, TEM and SEM. Furthermore, the catalytic activity of the catalyst was investigated for the oxidation of sulfides, oxidative coupling of thiols and synthesis of 5-substituted 1*H*-

tetrazoles. The Fe_3O_4@tryptophan@Ni nanocatalyst can be separated easily with an external magnet, and also it can be reused for several runs with little loss of activity. Excellent yields, easy preparation, low cost, eco-friendliness and chemical stability are the other advantages of the synthesized nanocatalyst.

ACKNOWLEDGEMENTS

The authors are deeply grateful to Erfan Ghadermazi and the University of Kurdistan for financial support of this research project.

ORCID

Nazanin Moeini http://orcid.org/0000-0001-7022-3734
Taiebeh Tamoradi http://orcid.org/0000-0002-8548-271X
Mohammad Ghadermazi http://orcid.org/0000-0001-8631-6361

REFERENCES

[1] M. A. Zolfigol, K. Amani, A. Ghorbani-Choghamarani, M. Hajjami, R. Ayazi-Nasrabadi, S. Jafari, *Catal. Commun.* **2008**, *9*, 1739.

[2] V. A. J. Silva, P. L. Andrade, M. P. C. Silva, A. B. Dominguez, L. J. AlbinoAguiar, J. A. Aguiar, *J. Magn. Magn. Mater.* **2013**, *343*, 138.

[3] V. Sokolova, M. Epple, *Angew Chem. Int. Ed.* **2008**, *47*, 1382.

[4] L. Shiri, A. Ghorbani-Choghamarani, M. Kazemi, *Aust. J. Chem.* **2016**, *69*, 585.

[5] R. A. Binin, R. F. Marques, F. J. Santos, J. A. Chaker, M. Jafelicci, *J. Magn. Magn. Mater.* **2012**, *324*, 534.

[6] A. Ghorbani-Choghamarani, M. Norouzi, *J. Mol. Catal. A* **2014**, *395*, 172.

[7] J. Liu, X. Peng, W. Sun, Y. Zhao, C. Xia, *Org. Lett.* **2008**, *10*, 3933.

[8] A. Ghorbani-Choghamarani, G. Azadi, *RSC Adv.* **2015**, *5*, 9752.

[9] M. Kazemi, L. Shiri, *J. Sulfur Chem.* **2015**, *36*, 613.

[10] K. Amani, M. A. Zolfigol, A. Ghorbani-Choghamarani, M. Hajjami, *Monatsh. Chem.* **2009**, *140*, 65.

[11] L. Shiri, A. Ghorbani-Choghamarani, M. Kazemi, *Aust. J. Chem.* **2017**, *70*, 9.

[12] A. Ghorbani-Choghamarani, Z. Darvishnejad, B. Tahmasbi, *Inorg. Chim. Acta* **2015**, *435*, 223.

[13] G. Chehardoli, M. A. Zolfigol, *Phosphorus Sulfur Silicon* **2009**, *185*, 193.

[14] A. Sarvary, A. Maleki, *Mol. Diversity* **2015**, *19*, 189.

[15] H. Sharghi, S. Ebrahimpour moghaddam, M. M. Doroodmand, *J. Organometal. Chem.* **2013**, *738*, 41.

[16] F. Abrishami, M. Ebrahimikia, F. Rafiee, *Appl. Organometal. Chem.* **2015**, *29*, 730.

[17] A. Ghorbani-Choghamarani, Z. Darvishnejad, M. Norouzi, *Appl. Organometal. Chem.* **2015**, *29*, 170.

[18] M. Nikoorazm, A. Ghorbani-Choghamarani, F. Ghorbani, H. Mahdavi, Z. Karamshahi, *J. Porous Mater.* **2015**, *22*, 261.

[19] J. C. Kim, H. X. Li, C. Y. Chen, M. E. Davis, *Micropor. Mater.* **1994**, *2*, 413.

[20] A. Corma, T. Rodenas, M. J. Sabater, *Chem. Sci.* **2012**, *3*, 398.

[21] A. Gao, M. Wang, J. Shi, D. Wang, W. Tian, L. Sun, *Appl. Organometal. Chem.* **2006**, *20*, 830.

[22] G. Aiping, W. G. Mei, W. Dongping, Z. Lu, L. Haibin, T. Wei, S. Licheng, *Chin. J. Catal.* **2006**, *27*, 743.

[23] M.-Y. Chen, L. N. Patkar, C.-C. Lin, *J. Org. Chem.* **2004**, *69*, 2884.

[24] A. Hasaninejad, G. Chehardoli, M. A. Zolfigol, A. Abdoli, *Phosphorus Sulfur Silicon* **2011**, *186*, 271.

[25] J. Bonnamour, C. Bolm, *Chem. – Eur. J.* **2009**, *15*, 4543.

[26] A. Kumar, R. Narayanan, H. Shechter, *J. Org. Chem.* **1996**, *61*, 4462.

[27] M. Nasrollahzadeh, Y. Bayat, D. Habibi, S. Moshaee, *Tetrahedron Lett.* **2009**, *50*, 4435.

[28] R. Dipak, Y. B. Patil, P. G. Wagh, K. Ingole, D. S. Singh, *New J. Chem.* **2013**, *37*, 3261.

[29] L. Lang, B. Li, W. Liu, L. Jiang, Z. Xu, G. Yin, *Chem. Commun.* **2010**, *46*, 448.

[30] H. Fu-She, *Chem. Soc. Rev.* **2013**, *42*, 5270.

[31] J. Montgomery, *Angew. Chem. Int. Ed.* **2004**, *43*, 3890.

[32] A. G. Davies, *Appl. Organometal. Chem.* **1998**, *12*, 878.

[33] A. Saxena, A. Kumar, S. Mozumdar, *J. Mol. Catal. A* **2007**, *269*, 35.

[34] L. Shiri, A. Ghorbani-Choghamarani, M. Kazemi, *Res. Chem. Intermed.* **2017**, *43*, 2707.

[35] A. Ghorbani-Choghamarani, G. Azadi, *Appl. Organometal. Chem.* **2016**, *30*, 247.

[36] A. Ghorbani-Choghamarani, B. Tahmasbi, P. Moradi, N. Havasi, *Appl. Organometal. Chem.* **2016**, *30*, 619.

[37] A. Ghorbani-Choghamarani, B. Ghasemi, Z. Safari, G. Azadi, *Catal. Commun.* **2015**, *60*, 70.

[38] T. Tamoradi, A. Ghorbani-Choghamarani, M. Ghadermazi, *New J. Chem.* **2017**, *41*, 11714.

[39] A. Ghorbani-Choghamarani, M. Norouzi, *J. Magn. Magn. Mater.* **2016**, *401*, 832.

[40] T. Tamoradi, A. Ghorbani-Choghamarani, M. Ghadermazi, *Polyhedron* **2018**, *145*, 120.

[41] T. Tamoradi, M. Ghadermazi, A. Ghorbani-Choghamarani, *Appl. Organomet. Chem.* **2018**, *32*, e3974. https://doi.org/10.1002/aoc.3974

[42] A. Ghorbani-Choghamarani, L. Shiri, G. Azadi, *RSC Adv.* **2016**, *6*, 32653.

[43] M. Tajbakhsh, M. Farhang, R. Hosseinzadeh, Y. Sarrafi, *RSC Adv.* **2014**, *4*, 23116.

[44] A. M. I. Jayaseeli, S. Rajagopal, *J. Mol. Catal. A* **2009**, *309*, 101.

[45] M. Nikoorazm, A. Ghorbani-Choghamarani, H. Mahdavi, S. M. Esmaeili, *Micropor. Mesopor. Mater.* **2015**, *211*, 174.

[46] S. M. Islam, A. S. Roy, P. Mondal, K. Tuhina, M. Mobarak, J. Mondal, *Tetrahedron Lett.* **2012**, *53*, 127.

[47] M. Darabi, T. Tamoradi, M. Ghadermazi, A. Ghorbani-Choghamarani, *Transition Met. Chem.* **2017**, *42*, 703.

[48] A. Ghorbani-Choghamarani, P. Moradi, B. Tahmasbi, *RSC Adv.* **2016**, *6*, 56458.

[49] A. Ghorbani-Choghamarani, P. Moradi, B. Tahmasbi, *RSC Adv.* **2016**, *6*, 56638.

[50] M. Abdollahi Alibeik, A. Moaddeli, *New J. Chem.* **2015**, *39*, 2116.

[51] A. Ghorbani-Choghamarani, M. Hajjami, H. Goudarziafshar, M. Nikoorazm, S. Mallakpour, F. Sadeghizadeh, G. Azadi, *Monatsh. Chem.* **2009**, *140*, 607.

[52] T. Tamoradi, M. Ghadermazi, A. Ghorbani-Choghamarani, *New J. Chem.* **2018**, *42*, 5479.

[53] G. Azadi, A. Ghorbani-Choghamarani, L. Shiri, *Transition Met. Chem.* **2017**, *42*, 131.

[54] M. Nikoorazm, A. Ghorbani-Choghamarani, M. Khanmoradi, *Appl. Organometal. Chem.* **2016**, *30*, 705.

[55] S. S. Ghodsinia, B. Akhlaghinia, *RSC Adv.* **2015**, *5*, 49849.

How to cite this article: Moeini N, Tamoradi T, Ghadermazi M, Ghorbani-Choghamarani A. Anchoring Ni (II) on Fe_3O_4@tryptophan: A recyclable, green and extremely efficient magnetic nanocatalyst for one-pot synthesis of 5-substituted 1*H*-tetrazoles and chemoselective oxidation of sulfides and thiols. *Appl Organometal Chem*. 2018; e4445. https://doi.org/10.1002/aoc.4445